27
8-1-78
25 to NTIS

ORNL/TM-6334

MASTER

Effects of Alternate Fuels Report No. 6
Analysis of Low-Alumina Castable Refractory Degraded by Residual Oil Combustion Products

G. C. Wei
V. J. Tennery

OAK RIDGE NATIONAL LABORATORY
OPERATED BY UNION CARBIDE CORPORATION · FOR THE DEPARTMENT OF ENERGY

DISTRIBUTION OF THIS DOCUMENT IS UNLIMITED

DISCLAIMER

Printed in the United States of America. Available from
National Technical Information Service
U.S. Department of Commerce
5285 Port Royal Road, Springfield, Virginia 22161
Price: Printed Copy $4.50 ; Microfiche $3.00

ORNL/TM-6334

Contract No. W-7405-eng-26

METALS AND CERAMICS DIVISION

MASTER

EFFECTS OF ALTERNATE FUELS
REPORT NO. 6
ANALYSIS OF LOW-ALUMINA CASTABLE REFRACTORY DEGRADED BY RESIDUAL OIL COMBUSTION PRODUCTS

G. C. Wei and V. J. Tennery

Date Published: July1978

Prepared for
Division of Industrial Energy Conservation
Department of Energy

NOTICE This document contains information of a preliminary nature. It is subject to revision or correction and therefore does not represent a final report.

OAK RIDGE NATIONAL LABORATORY
Oak Ridge, Tennessee 37830
operated by
UNION CARBIDE CORPORATION
for the
DEPARTMENT OF ENERGY

DISTRIBUTION OF THIS DOCUMENT IS UNLIMITED

THIS PAGE

WAS INTENTIONALLY

LEFT BLANK

CONTENTS

THIS PAGE

WAS INTENTIONALLY

LEFT BLANK

LIST OF FIGURES

LIST OF TABLES

EFFECTS OF ALTERNATE FUELS
REPORT NO. 6
ANALYSIS OF LOW-ALUMINA CASTABLE REFRACTORY DEGRADED BY RESIDUAL OIL COMBUSTION PRODUCTS

G. C. Wei and V. J. Tennery

ABSTRACT

This is the sixth of a series of reports on analyses of several types of refractories used in industrial furnaces with fuels considered alternate to natural gas. Analyses were performed on a low-alumina castable used for only two months in the roof of a residual-oil-fired boiler. The maximum hot-face temperature during operation was about 1530 K. The original microstructure of the castable, which consisted of mullite aggregate bonded with iron-containing gehlenite ($2CaO{\cdot}Al_2O_3{\cdot}SiO_2$), quartz and cristobalite, was totally altered during service in regions close to the hot face. At room temperature the altered microstructure consisted of corundum and gehlenite in a new oxide glass phase containing the elements Na, K, Ca, Fe, Ti, Al, Ni, and Si. The reactions of the fuel oil impurities Na, Fe, and Ni with mullite, quartz, and cristobalite in the original castable refractory caused the rapid degradation at the hot face during service in the boiler. Increasing the Al_2O_3 content of the castable by replacing mullite aggregate with alumina aggregate and using gehlenite with less iron impurity as the bonding material should improve the performance of this castable refractory or retard reactions of the castable with fuel oil combustion products including Na, Fe, and Ni.

INTRODUCTION

Diminishing supplies of natural gas[1] may necessitate a conversion from natural gas fuels to alternate fuels in a wide variety of industries in the U.S. in the forseeable future. Current favored industrial alternate fuels in the order of decreasing U.S. industrial interest are: distillate and residual oils, coal, electricity, and low-joule gases. Distillate oils are relatively clean and their effects on refractories are minor if the combustion system is properly installed and operated. The use of distillate oils in place of natural gas fuel has been adopted by many industrial firms. Residual oils offer an economic advantage over distillate oils in joules per dollar in many areas of the U.S., and therefore are viewed favorably as industrial alternate fuels. However, residual oils — essentially the remains of petroleum after gasoline and distillate extraction at various refinery stages — typically contain substantial impurities detrimental to refractories at high temperatures. Currently, industrial experience with residual oil combustion for process heat is inadequate to predict and prevent damage to the furnace linings. Therefore, analyses of refractories used in a residual oil combustion environment will provide a sound technical understanding of accelerated refractory and insulation degradation by reactions with residual oil impurities. Results of these analyses can guide the selection and development of refractories for improved service where use of this relatively impure fuel is desirable.

This report is the sixth of a series of reports on analyses of several generic types of refractories used in industrial furnaces fired with either residual oils or coal.[2-6] The refractory analyzed in this study is a low-alumina castable used in the roof of a residual-oil-fired boiler.

Castable refractories are mixtures of calcined fireclay or sintered alumina aggregate and finely ground cement.[7] Castables are applied as a wet, plastic mass by pouring, ramming, gunning, or vibration casting. The cement begins to set shortly after water is added and hardens after a prolonged drying period.[8,9] The dried material is then fired to produce a dense, monolithic structure. The procedures used to install, hydrate, set, dry, and fire castables are usually established empirically.

The advantages of using castable refractories are numerous. For example, joints, sources of spalling and liquid intrusion, are eliminated, and installation labor is reduced. In addition, under certain conditions castables are less permeable than refractory brick structures of similar composition, and consequently better resist penetration by liquids and gases at high temperatures. Refractory castables are used in numerous industries including petrochemical. Their applications include linings in boilers, process heaters, catalytic reactors, regenerators, coolers, and cyclones.[10] The castable refractories so applied have generally been used in a clean combustion environment typical of natural gas firing. Little open literature exists on the behavior of castable refractories exposed to high-temperature combustion of residual oils or coal. We believe this report is the first published analysis of refractory castables degraded by residual oil combustion products.

SPECIMEN HISTORY

The low-alumina castable we received from a chemical company had been used for only two months in the roof of a No. 6 oil-fired boiler. Figure 1 shows the gross fluxing and darkening that had occurred in regions of the refractory near the hot face. The maximum hot-face temperature reported by the chemical company was 1530 K, lower than the vendor-quoted maximum service temperature, 1580 K, for this type of castable. This temperature was estimated by boiler operators from their past experience and was considered accurate to ±30 K. As the No. 6 fuel oil used in firing the boiler was not analyzed for impurities, we do not know how much of them was introduced to the boiler during the exposure period.

RESULTS

The low-alumina castable was examined by chemical, x-ray diffraction, optical microscopy, electron microprobe, and scanning electron microscopy (SEM) analyses. The experimental procedures were the same as those outlined in a previous report.[2]

Visual inspection of the low-alumina castable specimen shown in Fig. 1 revealed two zones. The zone close to and including the hot face had completely changed color from the refractory's original brown-gray-pink hue to a very dark gray. Some glassy appearing slag had also formed on the hot face. This zone was designated the altered zone. Behind the altered zone was the unaltered zone of the refractory, which apparently had not undergone any drastic structural or color changes during use. The unaltered zone had a brown-gray-pink color.

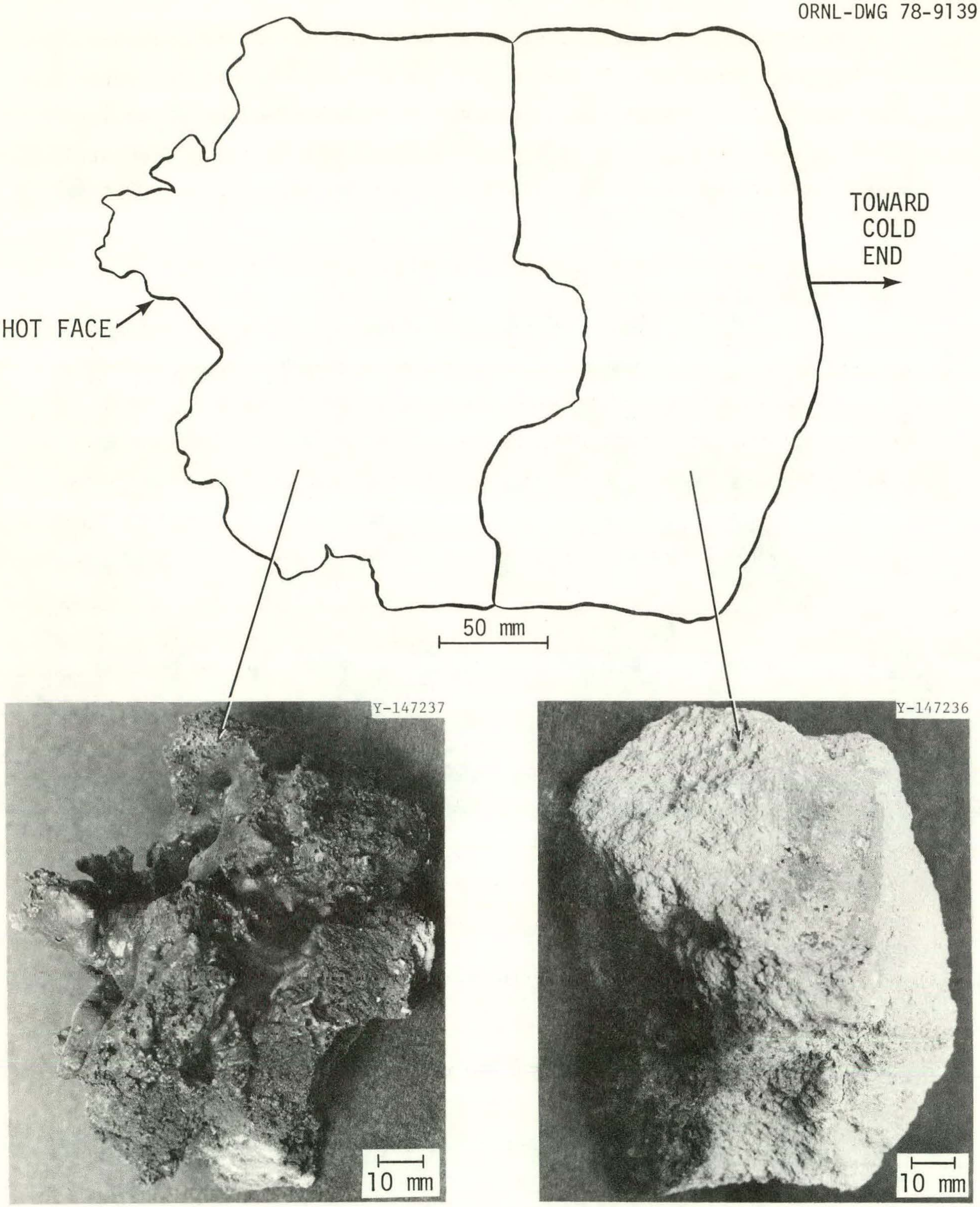

ALTERED ZONE

UNALTERED ZONE

Fig. 1. The Low-Alumina Castable Used in the Roof of a Residual-Oil-Fired Boiler for Two Months.

The results of chemical analyses of the altered and unaltered zones are shown in Table 1. The large value for loss-on-ignition in the unaltered zone is significant. This indicates that the plasticizing additive and water in the as-placed castable had not been completely burned off during the drying and curing of the castable and the first firing of the boiler. The Al_2O_3/SiO_2, CaO/Al_2O_3, and CaO/SiO_2 ratios are essentially the same in the altered and unaltered zones. The Fe_2O_3, Na_2O, and NiO contents increased significantly in the altered zone, probably because of Fe, Na, and Ni impurities in the fuel oil. Other impurities common to residual oils such as vanadium and sulfur, were present in the altered zone in only negligible amounts. The K_2O content in the altered zone was almost the same as that in the unaltered zone.

X-ray diffraction analysis of the altered and unaltered zones of the castable revealed mullite, low-cristobalite, and gehlenite, $2CaO \cdot Al_2O_3 \cdot SiO_2$. Rutile ($TiO_2$) and hematite ($Fe_2O_3$) were also present in minor amounts in both the altered and the unaltered zones. Alpha-quartz, observed in the unaltered zone of the refractory, apparently had been

Table 1. Chemical Compositions of the Altered and Unaltered Zones of the Low-Alumina Castable

Oxide	Weight Percent of Oxide Equivalent	
	Altered Zone	Unaltered Zone
Al_2O_3	37.3	33.5
CaO	13.6	11.5
Cr_2O_3	0.23	0.25
Fe_2O_3	6.13	5.85
K_2O	1.24	1.29
MgO	1.22	1.57
Na_2O	0.27	0.08
NiO	0.102	0.032
PbO	[a]	0.01
SO_3	0.027	0.22
SiO_2	38.3	34.2
TiO_2	1.62	1.60
V_2O_5	[a]	[a]
Loss on ignition	0	9.72

[a] None detected.

converted to either low-cristobalite or a glassy phase in the altered zone. Corundum was absent in the unaltered zone but was observed in the altered zone. Large grog particles in the unaltered zones contained mullite and low-cristobalite. The major crystalline phases identified in the altered and unaltered zones, and in the grog particles of the unaltered zone are listed in Table 2. Appendix A lists the x-ray diffraction data for these phases in terms of lattice spacings.

Table 2. Major Crystalline Phases in the Used Low-Alumina Castable

	Altered Zone	Unaltered Zone	Grog Particles in Unaltered Zone
Mullite	x	x	x
Low cristobalite	x	x	x
$2CaO \cdot Al_2O_3 \cdot SiO_2$	x	x	
Corundum	x		
α-quartz		x	
Rutile	x	x	
Hematite	x	x	

Reflected-light optical microscopy analyses of the unaltered zone revealed a microstructure consisting of large grog particles composed of fine mullite crystallites bonded with fine low cristobalite in a matrix material of gehlenite ($2CaO \cdot Al_2O_3 \cdot SiO_2$), α-quartz, and a siliceous glassy phase containing Al, K, Ti, and Fe. The phases were identified by electron microprobe analysis of the polished samples examined in the optical microscope and by x-ray diffraction results. Figures 2 and 3 illustrate the typical unaltered-zone microstructure of this refractory.

The altered zone had a distinctly different microstructure than did the unaltered zone. The altered region contained long lathlike corundum crystals (⩾200 µm) dispersed in a matrix material that included gehlenite ($2CaO \cdot Al_2O_3 \cdot SiO_2$) crystals, a new siliceous glassy phase containing the elements Na, K, Al, Ca, Ti, Fe, and Ni, and a highly reflecting Al-Ti-Fe oxide compound. Figures 4, 5, and 6 show the features of the

Fig. 2. Reflected-Light Photomicrograph of the Unaltered Zone Showing Mullite Grog Particles (M) Bonded with a Matrix Material Containing Gehlenite, Quartz, and a Siliceous Glassy Phase. 50×.

Fig. 3. Reflected-Light Photomicrograph of the Unaltered Zone Showing Mullite Grog Particles (M) Bonded with a Matrix Material Containing Gehlenite, Quartz, and a Siliceous Glassy Phase. Highly reflecting phases are rutile and hematite. 100×.

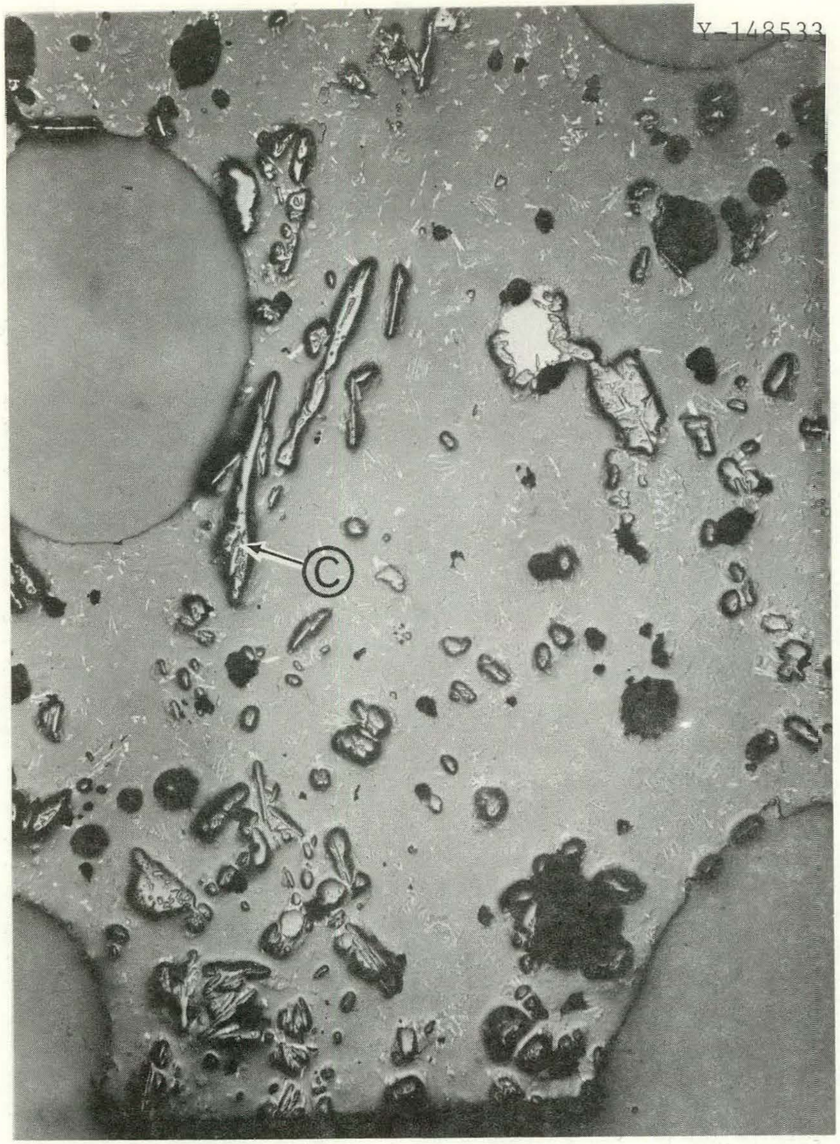

Fig. 4. Reflected-Light Photomicrograph of the Altered Zone Showing Long Corundum Crystals (C) Dispersed in a Matrix Containing Gehlenite and a New Siliceous Glassy Phase. 50×.

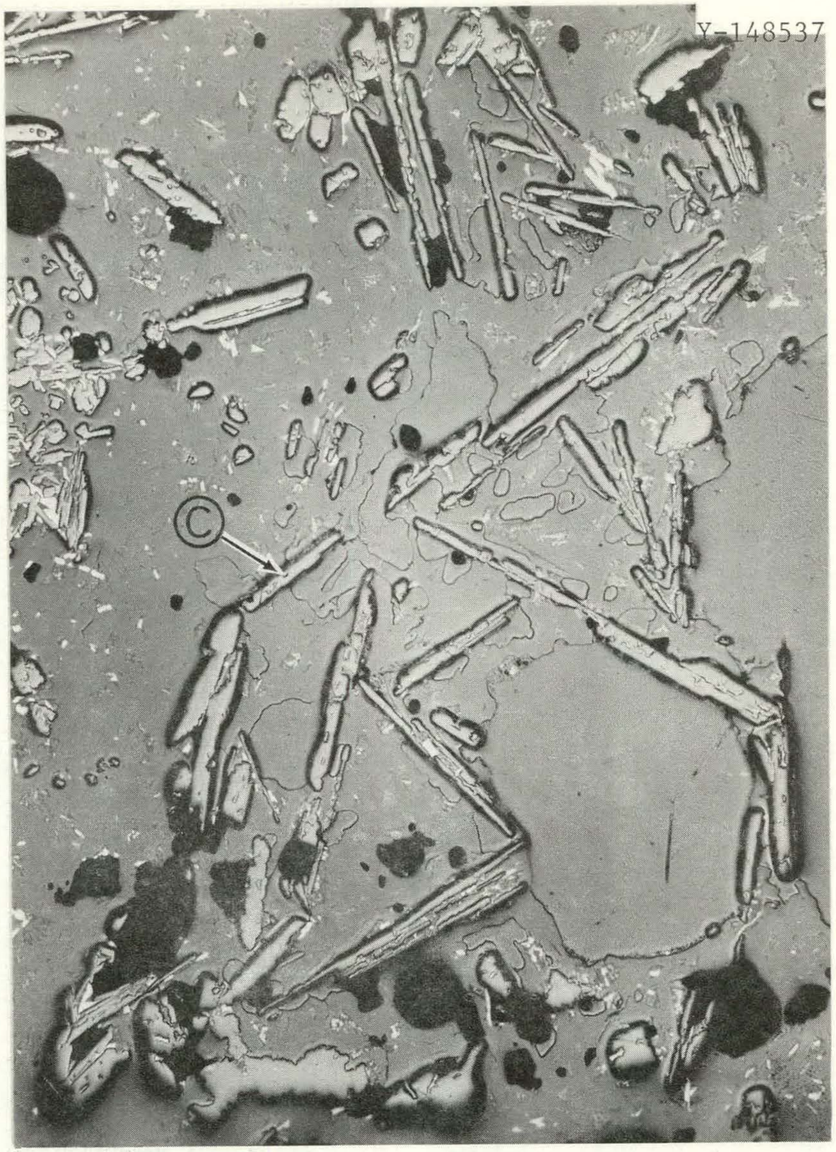

Fig. 5. Reflected-Light Photomicrograph of the Altered Zone Showing Long Corundum Crystals (C) Dispersed in a Matrix Containing Gehlenite and a New Siliceous Glassy Phase. Highly reflecting phase is an Al-Ti-Fe Oxide Compound. 100×.

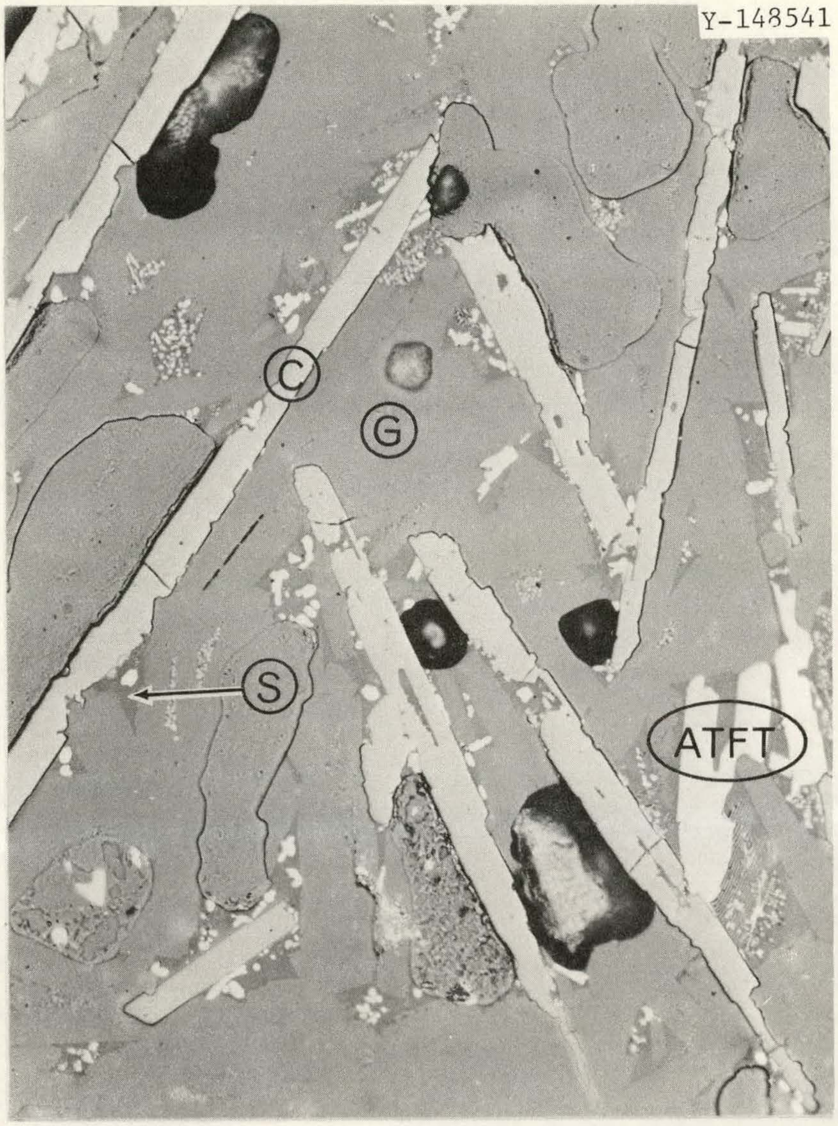

Fig. 6. Reflected-Light Photomicrograph of the Altered Zone Showing Long Corundum Crystals (C) in a Matrix Containing Gehlenite (G) and a New Siliceous Glassy Phase (S). Highly reflecting phase is an Al-Ti-Fe oxide compound (ATFT). 500×.

microstructure of the altered zone. The original mullite-containing grog particles in the castable were replaced by new phases. The original quartz grains were also absent. The irregular boundaries between the gehlenite and the new siliceous glassy phase make the gehlenite (M.P. 1866 K) appear to have started to dissolve in the siliceous glassy phase.

Scanning electron microscopy and energy dispersive x-ray analysis of the altered zone revealed the presence of nickel in the siliceous glassy phase of the altered zone. Figures 7, 8, and 9 illustrate the microstructural features of the internal pore surfaces of a fractured piece of the altered zone. Gehlenite crystals were embedded in the siliceous glassy phase, which contained the elements Na, K, Ca, Al, Ti, Fe, and Ni (Fig. 7). Figures 8 and 9 show small porous spheroidal particles, which probably were derived from the siliceous glassy phase. These objects contained the same elements as the glassy phase. The mechanism for the formation of these features was not identified. In the unaltered zone, many crystallites containing Ca, Al, Si, and apparently gehlenite were observed on the fractured surface (Fig. 10).

DISCUSSION

Fuel Oil Combustion Products

Since the residual oil used in firing the boiler was not analyzed for impurities, we do not know precisely either the types or amounts of impurities discharged from the fuel oil. However, comparison of the analytical results from the unaltered and altered zones of this low-alumina castable suggests that the elements observed in higher concentrations in the altered zone, or observed in the altered zone but not in the unaltered zone, came from the fuel oil and reacted with the refractory. This assumption implies that Na, Fe, and Ni were the more abundant fuel oil impurities during the service period for this refractory. Other impurities such as vanadium and sulfur commonly found in residual oils apparently were not present in significant quantities in the fuel oil used in firing the present boiler. If they were present, however, they did not react with the castable refractory, but left the boiler in the flue gases.

Degradation Mechanism

The degradation that had occurred in this low-alumina castable refractory mainly consisted of fluxing and structural alterations in

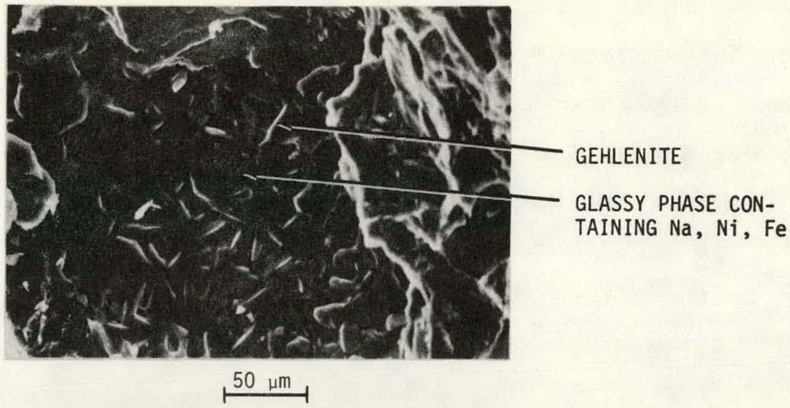

Fig. 7. Scanning Electron Micrograph of the Altered Zone Showing Gehlenite Crystals Embedded in a Glassy Matrix that Contains Elements Na, K, Ca, Ti, Fe, Al, Ni, and Si.

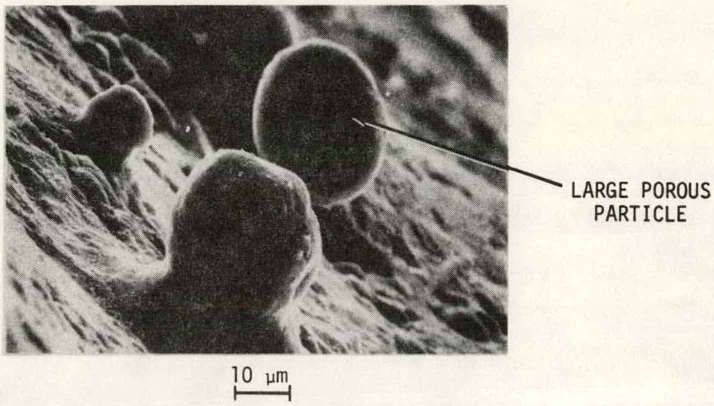

Fig. 8. Scanning Electron Micrograph of the Altered Zone Showing Large Porous Particles Containing Al, Si, K, Ca, Ti, Fe, and Ni Were Formed From the Hot Face of the Altered Zone.

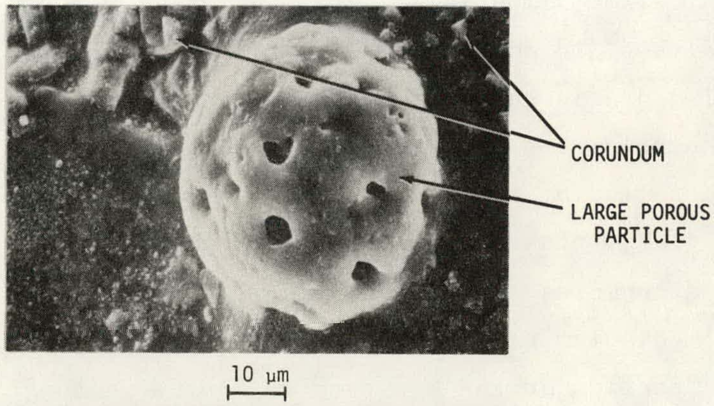

Fig. 9. Scanning Electron Micrograph of the Hot Face of the Castable Showing Large Porous Particle Formation and Small Crystallites Which Contain Mg, Al, Si, Ca, Ti, Fe, and Ni Distributed in a Glassy Matrix Containing Na, Al, Si, K, Ca, Ti, Fe, and Ni.

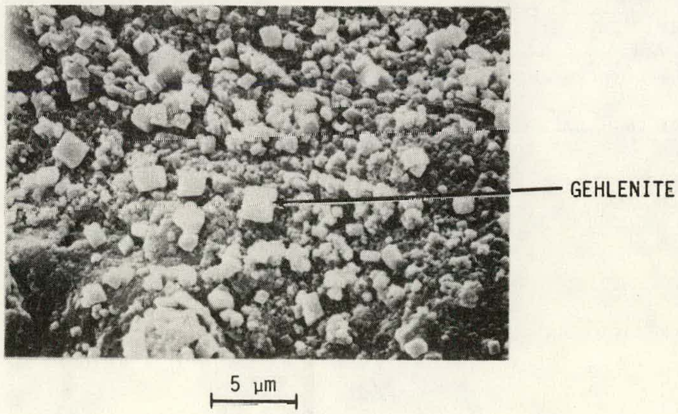

Fig. 10. Scanning Electron Micrograph of the Fractured Surface of the Unaltered Zone Showing Small Gehlenite Crystallites.

regions near the hot face. In this section we will discuss the degradation mechanism in terms of the microstructural, mineralogical, and chemical changes in the altered zone of the castable.

The optical microscopy analysis of the altered zone showed that during service in the boiler, cristobalite and mullite had essentially disappeared except for minor amounts detected by x-ray diffraction. Quartz was not observed in the altered zone by either optical microscopy or x-ray diffraction. Thus, quartz, cristobalite, and mullite, the major constituents of the original castable, reacted with the fuel oil impurities, primarily Na, Fe, and Ni, to form a new glassy phase in the altered zone during boiler operation. Corundum, in the form of long needles, crystallized from the newly formed glass melt in the altered zone. Gehlenite was present in both the altered and unaltered zones of the castable. Its concentration did not seem to be affected significantly by the residual oil combustion products, except for some evidence of dissolution in the new glass melt of the altered zone. The degradation in the altered zone, therefore, mainly resulted from reactions of quartz, cristobalite, and mullite with Na, Fe, and Ni fuel oil impurities.

Electron microprobe analyses did not reveal significant concentration gradients of the impurity elements in the various phases in the altered and unaltered zones. Consequently, the reactions causing refractory degradation appear to be controlled by transport at the interface between the original phases and the glassy phase that surrounds them, instead of by diffusion of detrimental species through the glassy phase in the altered zone. This type of mechanism requires that at operating temperatures, the rate of chemical reaction at the hot face of the refractory be significantly lower than the rate of diffusion of the impurity elements in the glass melt. It must also be lower than the generation rate of the glass melt itself at operating temperatures. To reduce the rate of refractory degradation, the slowest step of the degradation process must be retarded, that is, the chemical reaction rate must be decreased.

Composition Recommendations

Commercially available aluminosilicate castables can be divided into three major groups: high-alumina (>70 wt % Al_2O_3), intermediate-alumina (45–70 wt % Al_2O_3), and low-alumina (<45 wt % Al_2O_3). The castable we analyzed belongs to the last group. Either corundum or mullite grog particles are used as aggregate in all three families of aluminosilicate castables. The bond material consists of one or more of the following materials: calcium aluminate CA($CaO{\cdot}Al_2O_3$), gehlenite ($2CaO{\cdot}Al_2O_3{\cdot}SiO_2$), CA_2 ($CaO{\cdot}2Al_2O_3$), $C_{12}A_7$ ($12CaO{\cdot}7Al_2O_3$), gibbsite ($Al_2O_3{\cdot}3H_2O$), C_3AH_6 ($3CaO{\cdot}Al_2O_3{\cdot}6H_2O$), C_3AH_{8-12} ($3CaO{\cdot}Al_2O_3{\cdot}8\text{-}12H_2O$), quartz ($SiO_2$), mullite ($Al_2O_3$), pervoskite ($CaO{\cdot}TiO_2$), corundum ($\alpha$-$Al_2O_3$), and β-alumina. Frequently used bond systems consist of $CaO{\cdot}Al_2O_3$ and $3CaO{\cdot}Al_2O_3{\cdot}6H_2O$, $CaO{\cdot}Al_2O_3$ and $2CaO{\cdot}Al_2O_3{\cdot}SiO_2$, or $CaO{\cdot}Al_2O_3$ and $2CaO{\cdot}Al_2O_3{\cdot}SiO_2$ with appreciable Fe impurity.

The mullite originally present in this low-alumina castable reacted with the fuel oil impurities and resulted in corundum crystallizing from the glass melt in the altered zone. Therefore, aggregate-containing corundum should resist much better the corrosion and fluxing by fuel oil impurities than does aggregate consisting of mullite. Furthermore, increasing the Al_2O_3 content of the present castable by changing from mullite to alumina aggregate should improve the performance of the castable under operating conditions similar to those of this study.

The bond material, which was largely gehlenite in the present castable, seems to resist reasonably well reactions in which slag is produced by the fuel oil impurities. Thus, unless experiments demonstrate that other calcium aluminates such as CA or CA_2 withstand reactions with these fuel oil impurities better than gehlenite does, we recommend that gehlenite be used as the bonding material in a corrosive environment similar to that of this study. The original bonding material in the castable consisted of gehlenite with an appreciable level of iron impurities. Apparently, iron was dissolved in the glassy phase of the altered zone and either lowered the refractoriness of the castable or resulted in more liquid phase formation in the altered zone. Use of relatively iron-free gehlenite as the bonding material should result in less glass melt in the altered zone and retard the reactions of quartz, cristobalite, and mullite with fuel oil impurities.

We stress that because the castable degradation is a chemical reaction-controlled process, decreasing the rate of diffusion in the glass melt of the altered zone by increasing its Al_2O_3 content (by replacing the original quartz and cristobalite with mullite) probably will not effectively improve the performance of the castable. However, increasing the Al_2O_3 content in the glass melt may yield lower viscosity liquids and less glass phase, and may reduce the activity or chemical potential of detrimental species in the glass melt. Substitution of alumina aggregate for the original mullite aggregate should enhance the performance of the refractory because alumina is more stable than mullite in the specified environment.

CONCLUSIONS

A low-alumina (34 wt % Al_2O_3) castable refractory used in the roof of a residual-oil-fired boiler at a maximum hot-face temperature of 1530 K, underwent serious degradation. This resulted in boiler shutdown after a service time of only two months. This low-alumina castable was analyzed for the chemical, microstructural, and structural changes that accompanied the refractory degradation.

Quartz, cristobalite, and mullite in the original castable reacted with fuel oil impurities, including Na, Fe, and Ni, to form a new glass melt in the altered zone at operating temperatures. Corundum crystallized from the glass melt in the altered zone. Gehlenite, the bonding material in the original castable, apparently was not significantly affected by the fuel oil impurities. Rutile and hematite, present in minor amounts in the original castable, were also observed in the altered zone. In addition, an aluminum-titanium-iron oxide compound was formed in the altered zone.

Increasing the Al_2O_3 content of the castable by replacing mullite aggregate with alumina aggregate, and using gehlenite with a low level of iron impurity as the bonding material should improve the refractory performance of the castable for applications similar to the present case.

ACKNOWLEDGMENTS

The authors wish to thank the following Metals and Ceramics Division personnel for their contributions to the work described in this report: H. Keating for sample preparation; W. H. Warwick for ceramography; T. J. Henson for scanning electron microscopy; R. S. Crouse for electron microprobe work; and O. B. Cavin for x-ray diffraction. The authors are grateful to Gail Garbarini of the Division of Industrial Energy Conservation, DOE, for program sponsorship. The authors also express appreciation to C. S. Yust and C. S. Morgan of ORNL for reviewing the text of this report. This report was edited by N. Richards and prepared for publication by Connie Harrison.

REFERENCES

1. G. C. Wei and V. J. Tennery, *Impact of Alternate Fuels on Industrial Refractories and Refractory Insulation Applications, An Assessment,* ORNL/TM-5592 (September 1976).
2. G. C. Wei, L. A. Harris, and V. J. Tennery, *Effects of Alternate Fuels, Report No. 1, Analysis of High-Duty Fireclay Refractories Exposed to Coal Combustion,* ORNL/TM-5909 (December 1977).
3. G. C. Wei and V. J. Tennery, *Effects of Alternate Fuels, Report No. 2, Analysis of Basic Refractories Degraded by Residual Oil Combustion Products,* ORNL/TM-6088 (February 1978).
4. G. C. Wei and V. J. Tennery, *Effects of Alternate Fuels Report No. 3, Analysis of High-Duty Fireclay Refractories Degraded by Residual Oil Combustion Products,* ORNL/TM-6184 (April 1978).
5. G. C. Wei and V. J. Tennery, *Effects of Alternate Fuels Report No. 4, Analysis of Soaking Pit Cover Refractories Degraded by Residual Oil Combustion Products,* ORNL/TM-6204 (April 1978).
6. G. C. Wei and V. J. Tennery, *Effects of Alternate Fuels Report No. 5 — Analysis of Fused Cast AZS Refractory, Silica Refractory, and High-MgO Refractory Degraded by Residual Oil Combustion Products,* ORNL/TM-6278 (May 1978).
7. K. Shaw, *Refractories and Their Uses,* John Wiley and Sons, Inc., New York, 1972.

8. T. D. Robson, *High-Alumina Cements and Concretes*, John Wiley and Sons, Inc., New York, 1962.
9. C. Gleitzer, B. Courrier, G. Poirson, and J. G. Gourlaoueu, "The Use of Quantitative X-Ray Crystallographic Analysis in the Study of Refractories," *Trans. Br. Ceram. Soc.* 75(3): 61–67 (1976).
10. T. W. Smoot and G. D. Cobaugh, "Monolithic Refractories for Process Equipment," *Chem. Eng. NY* 72(17): 105–110 (1965).

APPENDIX A1

X-RAY DIFFRACTION DATA

THIS PAGE

WAS INTENTIONALLY

LEFT BLANK

Table A1. X-Ray Diffraction Data of the Altered Zone

Lattice Spacings, nm						
Altered Zone	Corundum	Mullite	$2CaO \cdot Al_2O_3 \cdot SiO_2$	Low-Cristobalite	Rutile	Hematite
0.65154						
0.64587						
0.48087						
0.46561						
0.40203				0.404		
0.39001						
0.37587			0.371			
0.36043						0.366
0.34662	0.3479					
0.34399		0.3428	0.343			
0.33448		0.3390				
0.32491					0.325	
0.31832				0.3138		
0.31104						
0.30298			0.307			
0.29402						
0.28865		0.2886	0.285			
0.28182				0.2845		
0.27985						
0.27183			0.272			
0.26465		0.2694				0.269
0.25460	0.2552	0.2542	0.2535			
0.25163						0.251
0.24947				0.249	0.2487	
0.24616						
0.24551			0.2435			
0.24295		0.2428				
0.24232						
0.24026			0.2404			
0.23787	0.2379					
0.23529						
0.23162						
0.22593		0.2292			0.2297	
0.22299						
0.21961			0.2195			0.220
0.21759						
0.21699	0.2165					
0.21526						
0.21390						
0.21337		0.2121	0.2126			
0.20872						
0.20826					0.2054	
0.20208				0.2024		
0.20144						
0.19811		0.1969	0.1967			
0.19263			0.1924			
0.18872						
0.18769			0.1864			
0.18354						0.184
0.17992		0.1795	0.175			
0.17956						
0.17664						
0.17399						
0.17313			0.1723			
0.17148						
0.17127						0.169
0.16014			0.1616			
0.15348						
0.15207			0.1519			
0.15099						
0.14856						
0.14750			0.1475			
0.14531						
0.14487			0.1437			
0.14120						
0.14060						
0.13872						
0.13750			0.1375			
0.13596			0.1361			
0.13407			0.1327			
0.12374			0.1253			

Table A2. X-Ray Diffraction Data of the Unaltered Zone

	Lattice Spacings, nm					
Unaltered Zone	Mullite	$2CaO \cdot Al_2O_3 \cdot SiO_2$	α-Quartz	Low-Cristobalite	Rutile	Hematite
0.53370		0.546				
0.49607		0.508				
0.47075						
0.42183		0.422	0.426			
0.40583				0.404		
0.34012	0.3428					0.366
0.33597	0.3390		0.3343			
0.33143					0.325	
0.30278		0.307		0.3138		
0.28639	0.2886	0.285		0.2845		
0.27223		0.272				
0.27127						
0.27039						0.269
0.26733	0.2694					
0.26710						
0.24913	0.2542			0.249	0.2487	0.251
0.24714						
0.24371	0.2428	0.2435	0.2456			
0.24113		0.2404				
0.22738	0.2292	0.2292	0.2281		0.2297	
0.22604						
0.22189			0.2236			
0.22147						0.220
0.21920		0.2195				
0.21118	0.2121	0.2126	0.2127			
0.21057	0.1969	0.2043	0.1979	0.2024	0.2054	
0.16899	0.1795	0.175				
0.16856					0.1687	0.169
0.16814						
0.16785		0.1632	0.1671			
0.15901		0.1616				
0.15155		0.1519				
0.14367		0.1437				

Table A3. X-Ray Diffraction Data of Grog Particles in the Unaltered Zone

Lattice Spacings, nm		
Grog Particles in the Unaltered Zone	Mullite	Low-Cristobalite
0.53756		
0.40730		0.404
0.34179	0.3428	
0.33784	0.3390	
0.31393		0.3138
0.28819	0.2886	
0.28435		0.2845
0.26873	0.2694	
0.25411	0.2542	
0.25075		0.249
0.24538		
0.24257	0.2428	
0.23470	0.2292	
0.22038		
0.21189	0.2121	
0.21024		
0.20247		0.2024
0.19637	0.1969	
0.17946	0.1795	
0.16945		
0.16896		
0.16007		
0.15252		
0.14435		

THIS PAGE

WAS INTENTIONALLY

LEFT BLANK

INTERNAL DISTRIBUTION

1–2. Central Research Library
3. Document Reference Section
4–5. Laboratory Records Department
6. Laboratory Records, ORNL R.C.
7. ORNL Patent Office
8. R. S. Crouse
9. R. G. Donnelly
10. J. I. Federer
11. C. B. Finch
12. T. G. Godfrey
13–15. M. R. Hill
16. W. J. Lackey
17–26. T. S. Lundy
27. D. L. McElroy
28. A. E. Pasto
29. H. Postma
30–39. V. J. Tennery
40. S. M. Tiegs
41. D. B. Trauger
42–51. G. C. Wei

EXTERNAL DISTRIBUTION

52. D. Allen
Southern Portland Cement Co.
P. O. Box 937
Victorville, CA 92305

53. R. W. Anderson
Diversified Insulation, Inc.
P. O. Box 188
Hamel, MI 55340

54. J. E. Bailey
Raw Materials Specialist
Ford Motor Company
Glass Technical Center
25500 West Outer Drive
Lincoln Park, MI 48146

55. B. H. Baker
ARMCO Steel Corp.
Res. Center South
Middletown, OH 45043

56. W. T. Bakker
Fossil Energy Div.
Department of Energy
20 Massachusetts Ave., NW
Washington, DC 20545

57. S. Banerjee
General Refractories Co.
P. O. Box 1673
Baltimore, MD 21203

58. L. Baumer
Ownes-Illinois, Inc.
P. O. Box 1035
Toledo, OH 43666

59. N. Bernoth
C-E Refractories Co.
Box 828
Valley Forge, PA 19482

60. J. M. Bevilacqua
The Carborundum Co.
P. O. Box 808
Niagara Falls, NY 14302

61. D. R. Bissell
Drexel Refractories Co.
Box 50
Kittanning, PA 16201

62. D. S. Blum
Quality Control Manager
Plibrico Company
1800 N. Kingsbury Street
Chicago, IL 60614

63. G. E. Brinkerhoff
Manager, Technical Services
A. P. Green Refractories
Company
Mexico, MO 65265

64. J. J. Brown
Dept. of Materials
Engineering
Virginia Polytechnic
Institute and State
University
Blacksburg, VA 24061

65. B. R. Brown
E. I. duPont de Nemours & Co.,
Inc.
1007 Market St.
Wilmington, DE 19898

66. F. Campbell
Babcock and Wilcox Co.
Box 923
Old Savanna Rd.
Augusta, GA 30903

67. A. N. Copp
Basic Refractories
(Sub. of Basic, Inc.)
845 Hanna Bldg.
Cleveland, OH 44115

68. J. A. Crookston
A. P. Green Refractories Co.
Green Blvd.
Mexico, MO 65265

69. C. R. Enoch
Resco Products, Inc.
Box 108
Norristown, PA 19404

70. W. X. Fay
General Refractories Co.
50 Monument Rd.
Bala-Cynwyd, PA 19004

71. M. P. Fedock
Assistant Division Head
Iron and Steelmaking Division
Republic Steel Corporation
Research Center
6801 Brecksville Road
Cleveland, OH 44131

72. L. E. Ferreira
Interpace Corporation
Corporate Headquarters
Box 1111
Parsippany, NJ 07054

73. R. E. Ferris
Kaiser Research Center
Box 870
Pleasanton, CA 94566

74–83. G. Garbarini
Division of Industrial
Energy Conservation
Department of Energy
20 Massachusetts Ave., NW
Washington, DC 20545

84. R. Grekrila
Research Center
Westinghouse Electric Corp.
Beulah Road
Pittsburgh, PA 15235

85. R. S. Harris
Anchor Hocking Company
Lancaster, OH 43135

86. D. Harvey
Department of Energy
20 Massachusetts Ave., NW
Washington, DC 20545

87. S. P. Hepburn
ICI Fiber Materials
Concord Pike and New
Murphy Road
Wilmington, DE 19849

88. R. H. Herron
Homer Research Laboratory
Bethlehem Steel Corporation
Bethlehem, PA 18017

89. A. V. Illyn
Babcock & Wilcox
P.O. Box 923
Augusta, GA 30903

90. H. L. Johns
Zircoa Products
31501 Solon Road
Solon, OH 44139

91. K. K. Kappmeyer
Applied Research Laboratory
United States Steel Corp.
Monroeville, PA 15146

92. R. V. Kilgore
Gunning Refractories Company
Box 38
Pedro, OH 45659

93. W. D. Kingery
Department of Materials
Science and Engineering
Massachusetts Institute of
Technology
Cambridge, MA 02139

94. L. Krietz
Plibrico Company
1800 N. Kingsburg Street
Chicago, IL 60614

95. L. J. Kuhlman
Monsanto Company
800 N. Lindberg Blvd.
St. Louis, MO 63166

96. R. G. LaBar
Alcoa Research Laboratories
Aluminum Company of America
Alcoa Center, PA 15069

97. R. A. Landy
Director of Research
North American Refractories
Company Research Center
Curwensville, PA 16833

98. J. Langensiepen
Brockway Glass Company
Central Laboratory
Brockway, PA 15824

99. R. Limes
Republic Steel Corporation
1441-T Republic Bldg.
P. O. Box 6778
Cleveland, OH 44101

100. C. Lindsay
Tennessee Valley Authority
303 Union Bldg.
Knoxville, TN 37902

101. D. E. McBride
Zircoa
31501 Solon Rd.
Box 39217
Cleveland, OH 44139

102. J. R. McGaughey
Bickley Furnaces, Inc.
550 State Road
Philadelphia, PA 19114

103. T. D. McGee
Iowa State University
Materials Science and
Engineering Department
Ames, IA 50010

104. R. W. Marshell
North American Manufacturing
Company
4455 E. 71st Street
Cleveland, OH 44105

105. F. M. Maupin
A. P. Green Refractories
Company
Green Blvd.
Mexico, MO 65265

106. W. Mead
Temtek-Allied Division
Ferro Corp.
One Erieview Plaze
Cleveland, OH 44114

107. E. D. Miller
Lava Crucible-Refractories
Company
1045 Oliver Bldg.
Pittsburgh, PA 15222

108. R. J. Moffat
Pullman-Swindell
441 Smithfield Street
Pittsburgh, PA 15222

109. J. E. Neal
Johns-Manville Corp.
Box 5108, Greenwood Plaza
Denver, CO 80217

110. R. Neeley
Chattanooga Glass Company
400 W. 45th Street
Chattanooga, TN 37410

111. J. A. Nelson
University of Illinois
Urbana, IL 61801

112. R. E. Nelson
C-E Minerals Company
901 E. 8th Avenue
King of Prussia, PA 19406

113. W. S. Netter
Monsanto Company
800 N. Lindbergh Blvd.
St. Louis, MO 63166

114. D. Olenchut
Jones and Laughlin Steel Corp.
3A, Gateway Center
Pittsburgh, PA 15230

115. H. Orr
Trane Thermal Company
Brook Road
Conshohocken, PA 19428

116. J. Osborne
Division of Industrial
  Energy Conservation
Department of Energy
20 Massachusetts Ave., NW
Washington, DC 20545

117. R. C. Oxford
Development Laboratory
Refractories Division
Babcock & Wilcox Company
P.O. Box 923
Augusta, GA 30903

118. P. Papa
Cornhart Refractories Co.
1600 W. Lee Street
Louisville, KY 40210

119. J. D. Parsons
Chicago-Wellsville Fire
  Brick Company
1467 Elston Ave.
Chicago, IL 60622

120. C. M. Pelanne
Johns-Manville Corp.
Box 5108
Denver, CO 80217

121. S. C. Porter, Jr.
Globe Refractories Co.
(Div. of C-E Refractories Co.)
Box D
Newell, VA 26050

122. G. V. Prible
C-E Refractories Co.
(Div. of Combustion
  Engineering, Inc.)
Box 828
Valley Forge, PA 19482

123. R. Ramey
Inland Steel Research
3001 East Columbus Drive
East Chicago, IN 46312

124. P. H. Reed
New Castle Refractories Co.
Box 471
New Castle, PA 16103

125. D. M. Rice
Davis Fire Brick Co.
Box 235
Oak Hill, OH 45456

126. R. Rose
H. K. Porter Co.
Porter Bldg.
601 Grant St.
Pittsburgh, PA 15219

127. R. P. Ross
Glasrock Products, Inc.
2210 Marietta Blvd., NW
Atlanta, GA 30318

128. G. R. Rowland
Hartford Refractories,
  Emhart Corp.
P. O. Box 2809
Hartford, CT 06101

129. C. K. Russell
Res. Center
United States Steel Corp.
125 Jamison Lane
Mail Stop 43
Monroeville, PA 15146

130. E. C. Sargent
Kolb Refractories Co.
Box 95
East Greenville, PA 18041

131. B. L. Schmidt
Anchor Hocking Co.
Lancaster, OH 43130

132. F. E. Schmidt
E. I. DuPont de Nemours & Co., Inc.
Experimental Stations
Bldg. 304
Wilmington, DE 14898

133. R. L. Shultz
Armco Steel Corp.
Research Center South
Middletown, OH 45043

134. T. E. Smith
Southern Div.
Martin-Marietta Cement Co.
1800 Daniel Bldg.
Birmingham, AL 35223

135. W. J. Smothers
Homer Res. Labs.
Bethlehem Steel Corp.
Bethlehem, PA 18016

136. R. R. Smyth
FluiDyne Engineering Co.
5900 Olson Memorial Highway
Minneapolis, MN 55422

137. W. E. Swearingen
Koppers Co., Inc.
Pittsburgh, PA 15219

138. L. H. Sweet
Manager Technical Development
Carborundum Co.
P. O. Box 808
Niagara Falls, NY 14302

139. C. A. Taylor
Shell Oil Co.
1 Shell Plaza, Box 2463
Houston, TX 77001

140. C. H. Taylor
National Cruicible Co.
Queen St. and Mermaid Lane
Philadelphia, PA 19118

141. E. A. Thomas
Charles Taylor Div.
NL Industries, Inc.
8361 Broadwell Road
P. O. Box 44040
Cincinnati, OH 45244

142. L. J. Trostel, Jr.
Norton Co.
One New Bond St.
Worcester, MA 01606

143. B. S. Tucker
The Refractories Inst.
1102 One Oliver Plaza
Pittsburgh, PA 15222

144. M. L. Van Dreser
Center for Technology
Kaiser Aluminum and Chemical Corp.
Box 870
Pleasanton, CA 94566

145. R. F. Whitford
North American Refractories Co.
1012 National City E 6th Bldg.
Cleveland, OH 44114

146. R. D. Whiting
Coors Porcelain Co.
600 9th St.
Golden, CO 80401

147. J. R. Wilson
Shell Development Co.
Box 1380
Houston, TX 77001

148. J. Wosinsky
Corning Glass Works
Box 432
Corning, NY 14830

149. R. L. Yeckley
Industrial Market
Harbison-Walker Refractories
Division of Dresser Industries, Inc.
2 Gateway Center
Pittsburgh, PA 15222

150. S. Young
Babcock and Wilcox Refractories Co.
Old Savanna Rd.
Box 923
Augusta, GA 30903

151. C. E. Zimmer
Babcock and Wilcox Co.
Lynchburg, VA 24505

152–153. Research and Technical Support Division
Oak Ridge Operations Office
Department of Energy
P. O. Box E
Oak Ridge, TN 37830

154–180. Technical Information Center
P. O. Box 62
Oak Ridge, TN 37830

☆U.S. GOVERNMENT PRINTING OFFICE: 1978-740-190/139